Journal of Atmospheric and Solar-Terrestrial Physics 86 (2012) 56–64

Contents lists available at SciVerse ScienceDirect

Journal of Atmospheric and Solar-Terrestrial Physics

journal homepage: www.elsevier.com/locate/jastp

Rocket borne in-situ Electron density and Neutral Wind measurements in the equatorial ionosphere—Results from the January 2010 annular solar eclipse campaign from India

G. Manju*, R. Sridharan[1], Sudha Ravindran, M.K. Madhav Haridas, Tarun K. Pant, P. Sreelatha, S.V. Mohan Kumar

Space Physics Laboratory, Vikram Sarabhai Space Centre, Trivandrum 695022, India

ARTICLE INFO

Article history:
Received 29 December 2011
Received in revised form
20 June 2012
Accepted 21 June 2012
Available online 30 June 2012

Keywords:
Annular eclipse
Electron density
Neutral wind
Blanketing Es
Counter electrojet

ABSTRACT

One of the recent developments in the form of a novel probe for simultaneous in-situ measurements of Electron density and Neutral Wind (ENWi) parameters was extensively made use of during the annular solar eclipse that passed right over the magnetic dip equatorial station, Trivandrum in India. The response of the equatorial ionosphere to the annular solar eclipse of January 2010 is investigated using the data from ENWi and other ground based instruments like digital Ionosonde, HF radar, magnetometer etc. Significant effects on the neutral wind components and electron densities during the peak phase of the eclipse are brought out by the ENWi data. A clear reversal in the zonal neutral wind is observed during the rocket flights at the peak phase of the eclipse as well as in the flight conducted 3 h later. The ground magnetic field measurements revealed the reversal of electrojet during the eclipse alongwith blanketing Es layers vindicating the earlier hypothesis that blanketing Es layers manifest over magnetic equatorial regions only during periods of either weak or reversed electrojet (counter electrojet). The HF radar results independently substantiate the in situ measurements with regard to the location of the irregularities and their Doppler velocities. The regional scale changes that have been brought about by the Solar eclipse both in the neutral and ionized medium and the consequent electrodynamics are highlighted.

© 2012 Published by Elsevier Ltd.

1. Introduction

Neutral winds and plasma densities are two important parameters, especially in the equatorial upper atmosphere, as they control/modulate all the major geophysical phenomena in this region. The upper atmospheric structure, energetics and dynamics are strongly influenced by the solar radiation and hence are altered significantly during solar eclipses. The sudden cutoff of the solar insolation during a solar eclipse produces significant effects on the entire terrestrial atmosphere. These effects are expected to be all the more significant in modulating the equatorial electro-dynamical processes during a very rare phenomenon when the path of maximum obscuration falls right on the magnetic equator that too during noon hours. Several researchers in the past, have investigated the response of the ionosphere to solar eclipses (Klobuchar and Whitney, 1965; Afraimovich et al., 1998; Muller-Wodarg et al., 1998; Sridharan et al., 2002; Chandra et al., 2007; West et al., 2008; Le et al., 2009, and the references cited in them). Nevertheless, the response of ionosphere over the magnetic equator and the adjoining low latitude regions has not been extensively studied for want of a suitable event occurring right over the equator. Hence the rare annular solar eclipse of 15 January 2010, with its maximum obscuration at ~1315 IST provided a unique opportunity to examine the eclipse induced effects on the equatorial electrojet (EEJ) and associated phenomena around local noon when all the equatorial electro-dynamical processes are expected to be in their full strength.

So far, direct measurements of the neutral winds in the lower thermosphere could be made through alkali vapour release/TMA release experiments (Larsen, 2002). This technique has the limitation of being restricted only to twilight and in the case of TMA could even be extended to night time conditions. There had also been attempts to conduct Lithium releases during day time conditions since the background continuum in the band of its resonant scattering is significantly low and using special detection techniques one could improve the signal–noise ratio but with little success from equatorial regions. Though the power of vapour release techniques have been amply demonstrated, the

* Corresponding author. Tel.: +91 471 2562597; fax: +91 471 2706535.
E-mail address: manju_spl@vssc.gov.in (G. Manju).
[1] Currently CSIR-ES at Physical Research Laboratory, Ahmedabad, 380009.

1364-6826/$ - see front matter © 2012 Published by Elsevier Ltd.
http://dx.doi.org/10.1016/j.jastp.2012.06.009

method is rather involved and the payloads are bulky in addition to the restrictions on the launch timings. The other technique viz., the meteor wind radar has a rather restricted range of 85–105 km only and the measurement is hampered by the presence of strong ionospheric irregularities in the crucial EEJ region. Further, ground based airglow spectroscopy cannot give altitudinal profiles and are generally restricted only to moonless periods of the night that too when the emissions intensities are favorable. Satellite based retrieval though is the best bet in the prevailing circumstances; it is well known that it suffers from poor spatial resolution. The above aspects are discussed in detail in Manju et al. (2012) and references therein. In this scenario, the simultaneous measurements of neutral winds along with plasma densities during a noon time annular solar eclipse over the magnetic equatorial regions made for the first time using a rocket borne Electron density and Neutral Wind (ENWi) probe are especially important. ENWi measurements have been made at unprecedented altitudinal resolution both on the eclipse day and on a control day in order to highlight the differences if any and to understand the causative mechanisms. The present note, while demonstrating the power of the measurement technique, brings out the significant changes that have been induced by the passing eclipse in the Mesosphere Lower Thermosphere (MLT) region. The changes that have been brought about in the neutral/ionized parts of the upper atmosphere and the consequent equatorial electrodynamics highlight that, the latter could be affected in more than one way that is generally believed to be applicable during quiet times. While mainly reporting the observations it is believed that the present note opens up newer avenues for possible interaction between the neutral and the ionized components of the MLT region and the consequent electrodynamics.

2. Basic principle of ENWi

In the E region of the ionosphere (90–120 km), the ion neutral collision frequency (ν_i) is very large as compared to the ion gyro frequency i.e., $\nu_i \gg \Omega_i$, while on the other hand the electron neutral collision frequency is dominated by the electron gyro frequency ($\nu_e \ll \Omega_e$). That is, the ions are essentially controlled by collisions with neutrals and they tend to move with the velocity of the neutrals, whereas the electrons are predominantly controlled by the magnetic field. Thus the neutral wind velocity and the ion drift velocity would be equal in this region. It is this principle that has been used for estimating the neutral wind velocity from the ENWi probe measurements. The photograph of the probe is shown in Fig. 1a and the rocket payload assembly showing the position of ENWi payload is shown in Fig. 1. The probe has two arms in the horizontal plane. Each arm has an outer tube maintained at ground potential. Insulated from this, is the field free drift tube, made up of stainless steel (SS) with both the ends flared out. Two grids (with $>96\%$ optical transmission) are welded to the flared-out ends of the SS tube. The drift tube assembly is maintained at a potential of -1 V. Just behind the inner end of the drift tube is the Faraday cup collector which collects the incoming ions that constitute the current. The cross-sectional view of one arm of ENWi is depicted in Fig. 2a.

A negative accelerating potential (-1 V) is applied to the entrance grid so that the ambient positive ions are drawn into the probe. These ions are then guided through the field free space inside the drift tube and finally reach the collector plate. The currents collected by the two collectors at the far inner ends of the two arms are independently measured. The applied potential imparts certain velocity ($\boldsymbol{V_i}$) to the ambient ions depending upon its mass and charge irrespective of the orientation of the probe. When the ambient ions, which are singly charged and are molecular in nature (with NO^+ and O_2^+ being the dominant species) in the E-region, are already drifting along with the neutral wind with a velocity $\boldsymbol{v_i}$, the velocity imparted due to the applied potential would get added up. When oriented in the velocity direction, one arm of the probe would encounter ions with velocity of $\boldsymbol{V_i}+\boldsymbol{v_i}$ while the opposite arm would encounter ions with $\boldsymbol{V_i}-\boldsymbol{v_i}$. The measured currents at both the arms would therefore be different and this difference would be proportional to the neutral wind velocity $\boldsymbol{v_i}$. Having an idea on the dominant ionic species in the E-region, the number density of the charged particles and also on the applied potential, an estimate of the neutral wind could be made at every instant and the altitude profile of the neutral winds could be built up as the rocket moves through the region.

The field of view of the instrument is the geometric field of view decided by the inlet aperture and the travel distance for the charged particles before they reach the collector plate. A narrow field of view of $\sim 10^\circ$ has been deliberately chosen so as to be able to demarcate the direction of measurements and to separate out the zonal and meridional components unambiguously when the

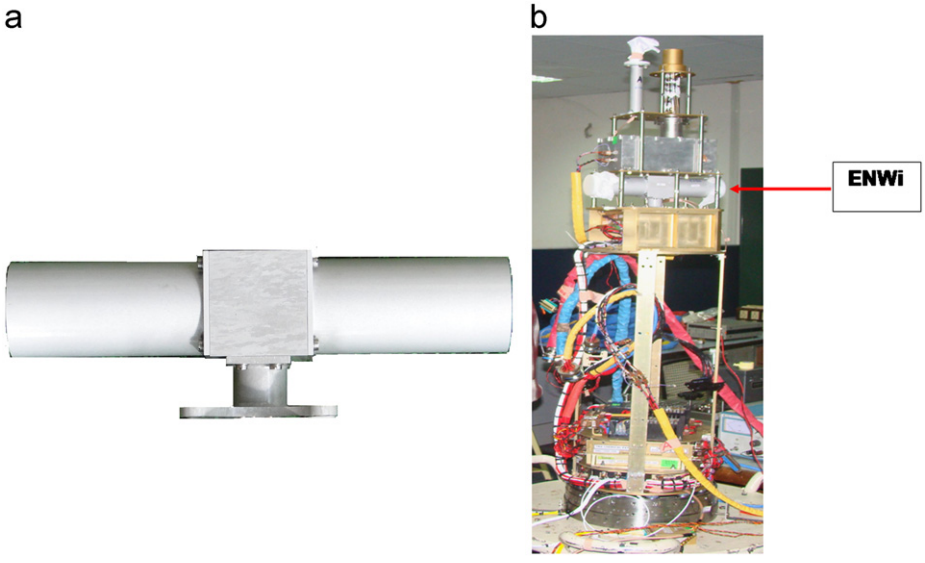

Fig. 1. (a) Photograph of ENWi payload and (b) photograph of rocket payload assembly indicating the position of ENWi probe.

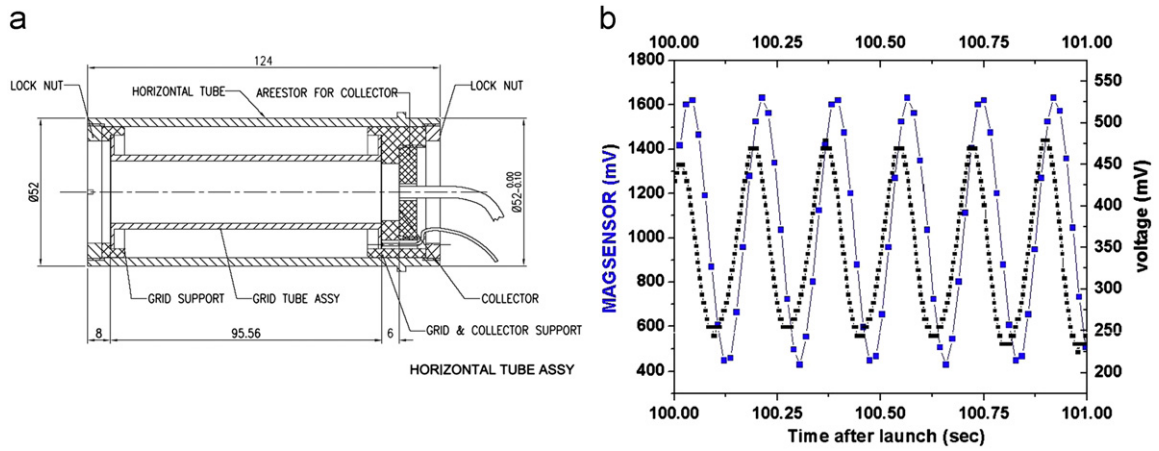

Fig. 2. (a) Cross-sectional view of one arm of ENWi and (b) sample magnetic sensor and voltage data for a duration of one second.

probe is mounted on a spinning platform like the top deck of a sounding rocket. We are eliminating spin effect by extracting data points only during the times when the probe is entirely in the E–W and N–S planes (so that no further smoothing is required), the direction being determined using spin information.

The data from the magnetic aspect sensor flown along with the payload is used to get the orientation of the probe in the horizontal plane. Using the spin rate information the wind values corresponding to the zonal and meridional directions are extracted. While the difference in the currents from both the arms is proportional to the neutral wind velocity, the sum of the currents from both the arms is directly proportional to the total ion density or in other words electron density ($N_i = N_e$) since, in this case the background neutral wind component gets subtracted. This situation is analogous to a DC probe. Since very low current measurements are involved, the frequency response of the amplifier is very critical. For this, an operational amplifier having very low input bias current typically of the order of 75 fA and an offset voltage of 0.15 mV is employed. The input circuit is well designed keeping all the above in mind. The rocket spin rate is $\sim$4 rps and the signal frequency is restricted with a low pass filter. We are not intending to look at small scale size irregularities which would put in an impracticable demand on the frequency response of the preamplifier. The output signal from one Faraday cup along with the magnetic sensor data for one second duration, is shown in Fig. 2.

Simultaneously obtained ground based digisonde data and SKiYMET meteor wind radar data are used to cross-calibrate the ENWi derived electron density and neutral winds respectively at least at some heights. The complete details of the probe with the first results and the experimental uncertainties such as photoelectric effect, wake effect, effect of launch elevation, ion Pedersen current effects and negative ion effects are discussed in Manju et al. (2012).

3. Results

3.1. Ground magnetic data

The ground based magnetic field data provide basic information on the prevailing geomagnetic conditions during the rocket experiments. The temporal variation of ΔH (the difference between the instantaneous horizontal component and the average night time value) from a nearby magnetic equatorial observatory, Tirunelveli, for the eclipse day (15/01/2010) along with that for the control day and the quiet day mean pattern (for a series of quiet days including control day) is shown in Fig. 3. The upward arrow in this and the subsequent figures indicate the time of maximum solar obscuration. Clearly there is strong development of electrojet up to 0900 h after which it showed a decreasing trend up to 1400 h, except for a brief increase around 1200 h. A strong counter electrojet (CEJ) with ΔH reaching $\sim$12 nT manifested on the eclipse day after 1400 h. The well established method of taking the difference in the ΔH values between a magnetic equatorial station and a station well away from the equator as representative of the electrojet strength has not been used for this event deliberately. The said approach is called for when one has to separate out local forcings from the global forcings like that of the Sq currents and the ring currents of magnetosphere origin on the electrojet. On a day when no significant ring current development is evident during the entire duration of the eclipse, ΔH TRV itself is a good measure of the electrojet strength. This condition is valid for both the eclipse day and the control day. Given the possibility of the generation of a counter Sq current system during the event under consideration as suggested by St. Maurice et al. (2010), presumably due to the eclipse induced changes in the neutral atmospheric dynamics, it is felt that ΔH TRV itself could be used in our study. To make the point more explicit the comparison of the magnetic data is now made with the mean ΔH variations from the same location for the period under consideration. The significant depression in

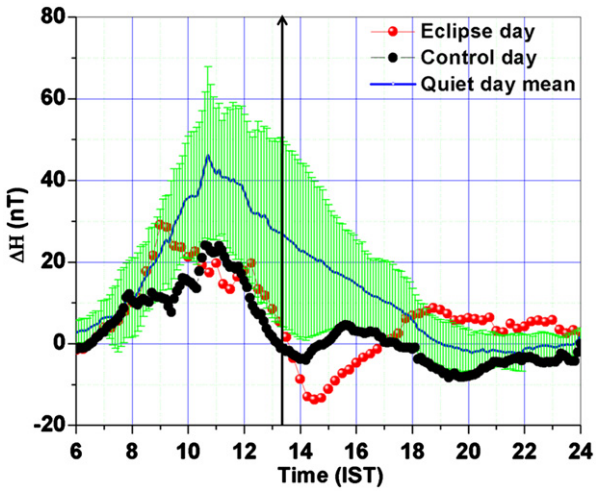

Fig. 3. Temporal variation of ΔH on the eclipse day (15.01.2010), control day (14.01.2010) and the mean quiet day pattern.

magnetic field below the night time level is very much evident in relation to quiet day mean which does not show excursion below night time level. It should also be kept in mind that the magnetic data is presented only to indicate the sort of changes the EEJ is undergoing and no quantitative assessment of the strength of the CEJ is attempted.

3.2. Electron density measurements

The ENWi probe was mounted along its axis on the top deck of the sounding rocket. With the effective launch elevation of 85 deg, the probe axis is nearly in the horizontal plane. The deviations if any would get reflected in the wind estimates. With its narrow field of view of ~10 deg, as the rocket spins, the probe would be sampling different look angles, enabling one to choose the zonal and meridional components with ease, with reference to the magnetic aspect sensor data. Detailed description of the experiments is provided by Manju et al. (2012). As mentioned earlier, the sum of the currents from both the arms at any instant would be proportional to the total charge particle density which, in this case, is the electron density. The altitude profile of the electron density is derived by summing the currents from both the arms. These are depicted in Fig. 4 for the eclipse day along with the control day pattern and the quiet day mean pattern. The quiet day mean electron density profile is a typical profile obtained at Thumba. It is obtained by averaging the profile obtained on 14 January 2010 and other available profiles from Thumba under similar solar activity conditions around noontime (Subbaraya et al., 1983). On the other hand, the profile during the peak of the annular eclipse shows significant differences. As expected, large decrease in the electron density is observed in the E region during the peak phase of the eclipse. This decrease is due to the sudden cut off of the solar insolation which results in the decrease of ionization due to dominance of chemical recombination. The densities were found to steadily increase right from 95 km, up to 110 km. A very interesting observation is the sharp nose like structure followed by a negative gradient at ~110 km. The profile showed a tendency to increase further above. Formation of a ledge of ionization around 110 km and the negative gradient that followed have important messages to convey and these aspects are discussed in the later section. On the whole, the significant differences between the two profiles are (i) Overall decrease in density due to lack of production and the continued loss due to recombination resulting in a decrease of electron density by a factor of ~4 at 95 km and more than 2, around 110 km and (ii) formation of a ledge of ionization ~110 km during the eclipse.

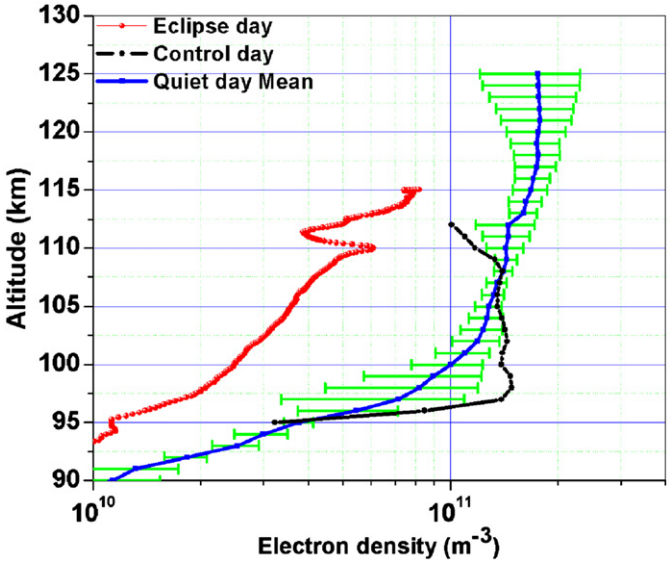

Fig. 4. Electron density profiles obtained from ENWi on the eclipse day (15.01.2010), control day (14.01.2010) and the mean quiet day pattern.

3.3. Electron density irregularities

The ENWi data had also been used to extract the characteristic features of the small scale irregularities. It is well known that the equatorial ionosphere is replete with plasma density irregularities due to the variety of plasma instability processes operating therein. The E-region of the ionosphere in the equatorial electrojet region during daytime is known to show two distinct types of irregularities viz., type I and type II, the former generated due to two stream instability and the latter due to gradient drift instability. These have been extensively discussed in the literature (Fejer and Kelley, 1980; Balsley et al., 1976; Farley and Balsley, 1973; Farley et al., 1981; Prakash et al., 1972). Characterizing these irregularities enables one to understand the basic drivers and the overall electro-dynamical processes. Extensive work has been done in these lines from India as well as from other locations (Prakash et al., 1972; Subbaraya et al., 1983).

A detailed study during specific events like the present one helps us to understand the response of the main drivers to the changes occurring during a solar eclipse. As a first cut exercise the entire electron density profile is obtained based on single arm data and the electron density data were available at around 120 m intervals. As the rocket moves closer to the apogee, it slows down and for the same spin rate; the altitudinal resolution would steadily increase. In order to emphasize medium scale irregularities of several hundred meters to kilometer scale sizes, that are responsible for affecting the radio communication, the electron density data were interpolated so that they are equally spaced, at every 200 m. This puts a limit on the smaller scale sizes that could be extracted; in this case it is >400 m. The data were de-trended so that scale sizes greater than 1 km were removed. Thereafter, wavelet analysis was carried out which yielded the power spectral output, for all the three flights (two on the eclipse day and one on the control day), in the scale sizes of 0.4–1 km (Fig. 5).

The significant differences in the altitude distribution of the power levels between the two rocket flights one on the eclipse day and another on the control day highlights to what extent the fundamental physical processes got altered during the eclipse. An independent cross check of the results from ENWi has been made by comparing them with the ground based coherent HF radar results for the same day and duration. The HF radar that operated at 18 MHz, gives information on the 8.3 m scale size irregularities. The MLT region of interest is sampled in 16 range bins. Though the scale sizes currently delineated from ENWi probe is in the range of 400–1000 m, the basic process that is responsible for their generation and the 8.3 m scale sizes recorded by the radar is the same and one would expect to see good one to one correlation in their altitude profiles. Fig. 6 depicts the normalized power of the irregularities in the range of 400–1000 m for ENWi probe and that corresponding to 8.3 m scale size inferred from the HF radar. The altitude resolution of HF radar is 3 km. Data in each panel is normalized with respect to the peak power considering all the three flights.

As expected the altitude region of the irregularities during the control day flight on 14th January 2010 is typical of a normal day and is restricted to the region of 95–100 km corroborated by the HF radar. It should be borne in mind that the HF radar has a poorer altitude resolution due to its finite pulse width. On the other hand, when we look at the eclipse day results of the ENWi probe corresponding to the maximum obscuration of the sun at 1305 h, the region of irregularities is shifted to 107–113 km and

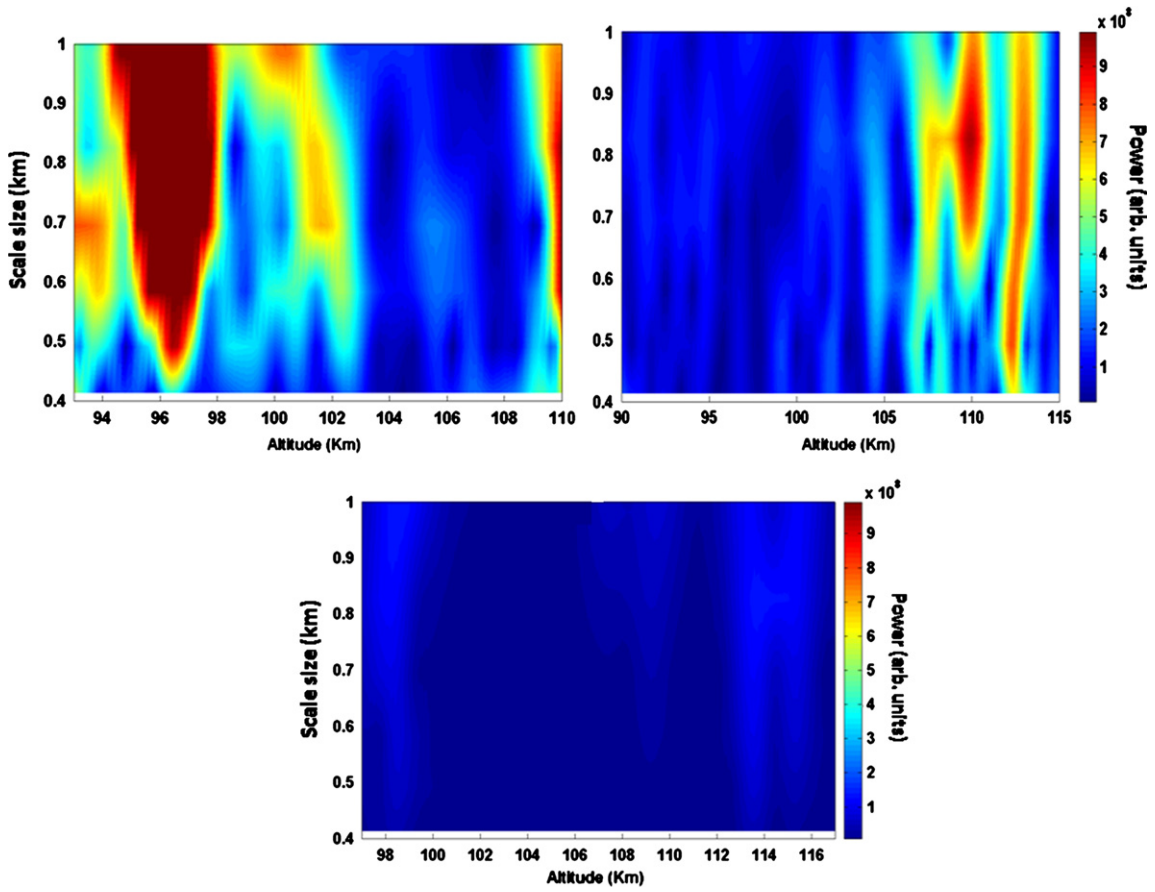

Fig. 5. Irregularity power spectrum for the medium range scale sizes (0.4–1 km) for three flights; top left: during the maximum obscuration phase of the eclipse, top right: corresponding to the control day (14.01.2010), and bottom: 1600 h flight on the eclipse day.

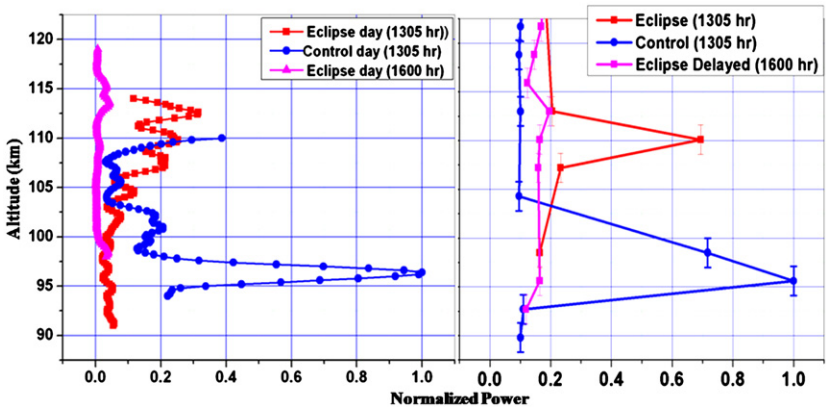

Fig. 6. Altitude profile of the normalized power for the three rocket flights (left panel) and the corresponding HF radar normalized backscattered power (right panel).

the HF radar too reveals exact one to one correspondence with the ENWi results. The third flight that was conducted at 1600 h on the eclipse day revealed no irregularities either in the ENWi or the HF radar. The distinctly different irregularity profiles indicate significant changes brought about by the eclipse and these would be discussed later.

3.4. Neutral wind components

The significant advantage of the ENWi probe had been in its ability to provide simultaneous measurements of the neutral wind components along with plasma densities in a critical region with unprecedented altitude resolution. For a comprehensive understanding of the equatorial processes in general, and the electro-dynamical processes like Equatorial Electrojet in particular, simultaneous measurements of both the neutral and ionospheric parameters are necessary and it is believed that the new ENWi probe has the potential to fill up an important gap area. The zonal and meridional wind components have been derived for the eclipse and the control days from the probe data and are presented below. Considering the sources of error in measurements mentioned in Manju et al. (2012), the measurement uncertainties pertaining to the instrument alone is estimated. It is seen that such errors amount to less than 10 m/s. For further quantification of the uncertainties, we plan to undertake more ENWi flights along with complementary experiments like TMA

releases so that a comprehensive estimate of the errors may be arrived at.

3.4.1. Zonal wind component

The control day, as expected on a typical day, showed zonal winds in the westward direction with a least velocity of $\sim$50 ms^{-1} around 100 km which monotonically increased to large values of $\sim$250 ms^{-1} around 110 km, which is the apogee of the sounding rocket (Figs. 7 and 8). When compared with satellite derived winds, the magnitudes inferred from ENWi data appear to be rather large. The experimental uncertainties including the various potential sources of errors and the seemingly large values for the zonal components on the control day have been discussed in the literature (Manju et al., 2012). Eclipse day pattern (Fig. 7), on the other hand, depicts a large reversal to eastward direction in the entire altitude range above 98 km. The wind magnitude had remained close to zero up to 97.5 km beyond which, there had been a buildup up to $\sim$105 km where in the magnitude had reached a value of $\sim$70 ms^{-1}. Higher above it had remained centered to this value up to the apogee of the rocket. Fig. 7 also shows the zonal wind profile from another flight conducted at 1600 h on the eclipse day with an aim to study the persistence of the eclipse effects if any. Incidentally, during this flight too the zonal winds had remained similar to the maximum obscuration time. The polarity of the wind had been eastward and varied from 50–100 ms^{-1} in the altitude region of 105–115 km. Thus, from the behavioral pattern of the zonal wind components, it could be seen that, that there is an eclipse induced effect in the form of reversal of the zonal winds, which could in turn have important ramifications as would be discussed later.

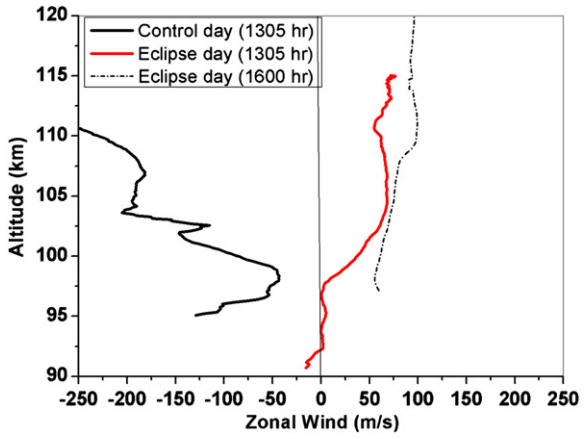

Fig. 7. Zonal winds derived from ENWi probe on eclipse day (15.01.2010) and control day (14.01.2010).

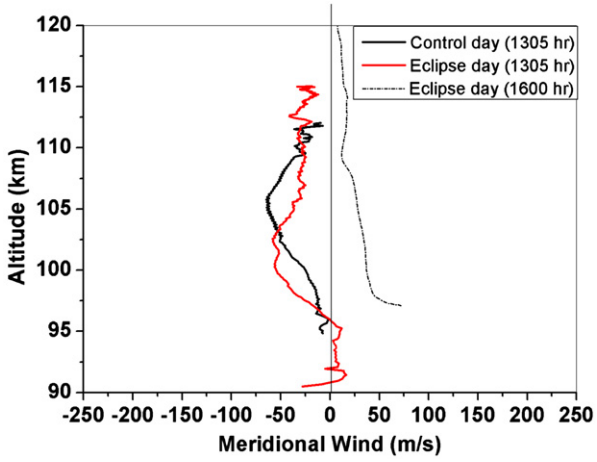

Fig. 8. Meridional winds derived from ENWi probe on eclipse day (15.01.2010) and control day (14.01.2010).

3.4.2. Meridional wind component

There had been hardly any change in the magnitude of the meridional winds from the control day to the eclipse day. On both the occasions the maximum of the wind had been 50 ms^{-1} and directed southward. There had been a shift in the altitude of maximum velocity from 105 km on the control day to 102.5 km on the eclipse day. On the other hand, the second rocket flight on the eclipse day at 1600 h registered a polarity reversal all through the altitude of measurements.

3.5. Irregularity phase velocity estimates

The HF radar located in Thumba, Trivandrum, operating at 18 MHz, has a beam swinging capability to three different directions like the west, zenith and east and, as mentioned earlier, was also operated to continuously monitor the changes brought about by the annular eclipse. Using the standard procedure (Tiwari et al., 2003; Manju et al., 2005), by making use of the Doppler information of the type II irregularities monitored by the radar, the line of sight phase velocities (V_p^θ) of the irregularities in the electrojet has been derived on the eclipse day and the control day (Fig. 9). Westward (eastward) drift of irregularities corresponds to an upward (downward) polarization electric field (Manju et al., 2005). The dotted lines in figure correspond to the absence of signal or non-availability of data. V_p^θ increased to a value of $\sim$60 ms^{-1} (westward) in the morning hours, but started to fall off to reach low values of $\sim$10 ms^{-1} (westward) close to noon time. Though the data are intermittent for want of sufficiently intense returns from the irregularities, the trend could be seen very clearly. By 1245 h, it is clear that V_p^θ has reversed to eastward direction attaining a maximum eastward value (30 ms^{-1}) at 1305 h, coinciding with the rocket experiment. Correspondingly the vertical polarization electric field also would have reversed to downward direction. Later on by 1320 h V_p^θ reverted back to its typical daytime polarities. It turns out that there was a clear reversal in the polarity of V_p^θ during 1245–1320 h, close to the peak eclipse phase, unlike on the control day, when no such polarity reversal is observed. Under normal circumstances over the magnetic equator, modeling studies have revealed that the vertical electric field would increase with altitude up to $\sim$120 km

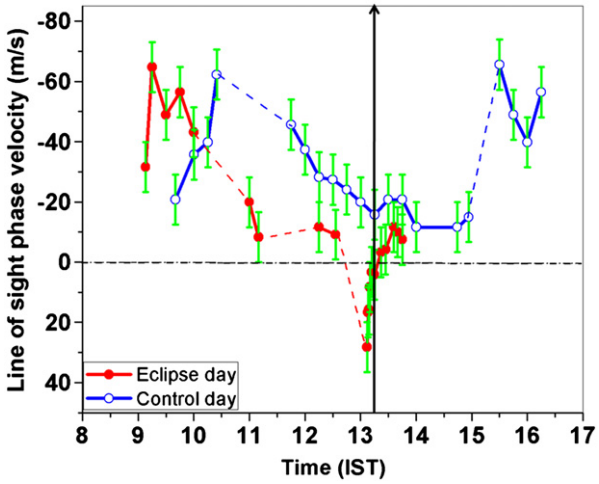

Fig. 9. Time variation of line of sight phase velocity of irregularities on eclipse day and control day.

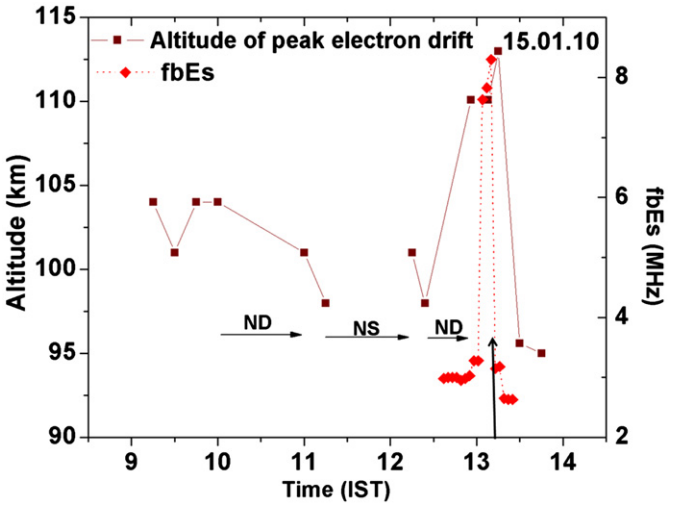

Fig. 10. Temporal variation of the altitude of peak electron drift and fbEs on the eclipse day.

and later steadily would decrease as the Pedersen mobility approaches the Hall mobility (Reddy, 1977). However, 2-D modeling studies by Anandarao et al. (1977) did show that the electric field tends to maximize only at the height of maximum velocity. When we critically analyze the altitude variation of the peak drift velocity during the eclipse, it is seen that the type II irregularity drift velocity maximized around 110 km on the eclipse day as shown in Fig. 10 which depicts the temporal variation of the altitude of the peak electrojet drift velocity as derived from the HF radar at Trivandrum. Though at the outset it may appear that the drift velocities have shown a tendency to maximize at higher altitudes, it is not possible to unequivocally make this statement because the drift velocity estimates are based on the radar returns from 8 m irregularities that get generated when the conditions are favorable i.e., when the electric field direction and the plasma density gradients are in the same direction. During the eclipse, since the electric field had already reversed its polarity, the irregularities could be generated only in the negative gradients of the electron density profile which in this case is located around 110 km. Though the magnitude of the drift velocity had been rather large (~30 m/s), due to want of irregularities lower below one cannot make an assessment of the velocities. It is seen that the back scatter returns come from the typical electrojet height region of 94–107 km prior to 1230 h while close to the peak phase of eclipse, strong signal returns are observed from altitudes centered ~110 km. From Fig. 6 it could also be noted that the received power from 110 km in this case is comparable to that at the EEJ maximum altitudes. This could mean that there had been very significant changes in the EEJ parameters during the eclipse. In the absence of complete information one has to necessarily infer based on the general picture. Normally the drift velocities maximize around noon (~50–60 m/s) and the typical velocity during similar conditions is ~20 m/s around 1300 h. On the eclipse day when one encounters a magnitude of 30 m/s under field reversed conditions, either it could be the maximum value or lower below it could even be larger. In the absence of any direct measurements no further insight could be obtained.

It is to be noted that, in the altitude region just above 110 km, the N_e profile on the eclipse day depicts, a clear negative electron density gradient. In the presence of downward directed electric field which has been substantiated by the radar results, the condition for generation of Gradient drift instability ($\Delta N \times E > 0$) (Prakash et al., 1972; Fejer and Kelley, 1980) is satisfied only in the region of 110–112 km. Around this time, a very strong blanketing Es layer is formed in the ground based ionosonde and the maximum frequency returned from this layer with time is also shown in the figure. It is very interesting to note that as the radar echoes grew in strength around 1300 h, blanketing E_s (E_{sb}) is observed in the Ionosonde, exactly coinciding with the strong echoes. The E_{sb} echoes were observed from ~1240 to 1325 h while the maximum obscuration occurred ~1315 h. The intense manifestation of E_{sb} had been rather short lived and lasted only for ~20 min in agreement with the field reversal duration. However, the maximum counter electrojet related magnetic field depression was observed much later ~1430 h. The location of irregularities and the associated sharp layer of ionization that manifested as blanketing E_s at a higher height viz., 110 km itself are rather unusual. The few available measurements during counter electrojet periods show that, customarily, the formation of a ledge is encountered around 92–94 km with the corresponding blanketing Es being detected by the ionosonde at those heights (Shirke and Sridharan, 1979 and the referenced therein). Only in one other case, reported by Manju and Viswanathan (2007), blanketing E_s related radar echoes were observed during CEJ at higher altitudes. The presence of a ledge of ionization providing negative gradients is a must for the gradient drift instability to operate, when the vertical field is pointed downwards. However, it is well established that though, the formation of such sharp ledges of ionization could easily be done over low and mid latitudes by wind shears, over the magnetic equator it is not possible due to the magnetic field lines being horizontal. Such restructuring of the ionization has to be necessarily done due to electrodynamical processes. It could be seen that the eclipse time measurements have revealed significant changes brought about in the MLT region, the ramifications of which need to be understood.

3.6. Discussion

It could be seen from the above presentation that the simultaneous measurements of neutral winds, plasma densities, ionization irregularities, and ground based radio probing by HF radar and Ionosonde along with ground magnetic data, as a part of an intense campaign to understand the effects induced by the annular solar eclipse in the equatorial ionosphere/thermosphere system have yielded rich dividends. The unique event with an obscuration of >84%, with its path of maximum obscuration lying just over the magnetic equator, that too during noon hours when all the equatorial geophysical processes would be in their full swing, provided a unique opportunity to study the impact of the eclipse. The promise shown by the newly developed ENWi (Manju et al., 2012) probe also comes to the fore based on the results obtained from it. When it comes to the plasma densities and the density irregularities, the probe had shown distinctly different density profiles which could be understood based on the chemical recombination of the dominant molecular ions in the near absence of the ionizing solar radiation. The recombination effects would be significantly larger in the lower heights and its effect is expected to decrease with altitude. As one moves to higher altitudes the transport effects would become dominant. The next critical observation pertains to the plasma density irregularities. As one would expect, on the control day, the medium scale irregularities that are primarily generated due to the gradient instability are located at the positive gradient when the vertical electric field is directed upward making it conducive for the instability to operate. This is a typical noon time condition over the magnetic equator. The HF radar confirms the presence of 8.3 m irregularities exactly in the same altitude region as detected by the ENWi probe. On the other hand, during the eclipse when the ground magnetometer had clearly shown the presence of a

counter electrojet, the primary field would have reversed resulting in the reversal of the vertical field to point downward. Both the conditions viz., the gradient which also had become shallow and also the field direction in the region where normally these irregularities are located, are not favourable for the generation of irregularities. The measurements both by ENWi and the HF radar confirm this aspect. However, at 110 km where a ledge of ionization is detected, one encounters a narrow height region with a negative altitudinal gradient. Kato (1973) attempted a one dimensional theory invoking electric fields generated due to gravity wave winds, to explain the stratifications seen in the evening and night time equatorial ionosphere. A 2-D analysis by Anandarao et al. (1977) demonstrated that the efficiency of the gravity wave winds is significantly less than what has been inferred by the 1-D calculations. In spite of this finding, the suggested mechanism by Kato (1973) could still be effective during evening and nighttime conditions when the recombination rate is slower when compared to the rate of convergence. The present measurements during a near total eclipse would take the E-region of the ionosphere more towards the evening conditions implying the possibility of gravity wave winds could have had a say in the formation of the ledge of ionization around 110 km. More detailed model calculations are called for to explain the observations. Further studies would address this aspect. Coming back to the negative gradient shown by the ledge of ionization, interestingly the irregularities are detected exactly in that height region by both the techniques. This would imply that the overall background and also the electro-dynamical conditions have gone through major changes during the eclipse which means that the main driver for the electrodynamics viz., the neutral winds should have undergone significant changes. Under normal circumstances the effects of neutral winds on EEJ over Indian longitudes have been studied in detail by earlier workers. Anandarao and Raghavarao (1987) have shown that the effects of horizontal winds and shears in them are felt only beyond 2 deg on either side of the magnetic equator while there had been very less change in the centre of the electrojet. While the zonal winds could alter the width of the electroject, the meridional winds could at the most shift the centre of the electrojet. Further, Raghavarao and Anandarao (1980) have demonstrated using their model that vertically downward winds, presumably of gravity wave origin, are capable of reversing the electrojet. Another independent study by Somayajulu et al. (1993) had shown very large changes in the zonal wind magnitudes associated with CEJs. On the other hand, studies on the occurrence pattern of the CEJs had shown that there exists a close coupling between the sudden stratospheric warming in the polar regions to the periodic occurrence pattern of the CEJs over the equator, making it into a global phenomenon (Stening et al., 1996; Vineeth et al., 2009). All the above only indicate the complexity of the phenomenon of CEJ and suggest that there could be more than one way by which it could be affected. The present results discussed in the paper bring out one more dimension to the problem of the reversal of the electrojet. The ENWi derived neutral winds do show in particular that the polarity and magnitude of the zonal winds have changed significantly during the eclipse. In all probability this could be localised and has a modulating effect on the normal Sq current system. The sudden cooling along the path of the eclipse right over the magnetic equator and the consequent changes brought about in the circulation pattern is believed to be responsible for the observed changes (St. Maurice et al., 2010). One of the recent studies during the same eclipse event using the unique multi wavelength dayglow photometer (Sumod et al., 2011), it had been shown that the mesosphere experienced a sudden warming during times of the eclipse which warrants significant changes in the wind pattern. It should also be noted that these results are just opposite of what had been shown earlier on many occasions (Vineeth et al., 2007) wherein the mesospheric regions had been shown to become cooler during CEJ. These differences highlight the point that the causative mechanisms for normal CEJ and the reversal experienced during this eclipse may be totally different and calls for an in depth study. As presented earlier, the measured zonal wind component has reversed from normal westward to eastward winds making it similar to what one encounters during night time conditions. On the other hand, it is noticed that the meridional components on both the control day and the eclipse day had been comparable. The effect of these changed wind patterns is expected to have a significant effect on the equatorial electrodynamics in general and the equatorial electrojet in particular. St. Maurice et al. (2010) in one of their studies have proposed that the relatively cooler temperatures along the path of the eclipse could trigger a low pressure system and result in some sort of a localized neutral dynamo altering the main global scale dynamo significantly in the region of the eclipse. Changes in thermospheric meridional wind pattern in the equatorial and low latitude F region, from equatorward during peak eclipse phase to strong poleward in post eclipse phase have been reported by Madhav Haridas and Manju (2012). Our observations do show significant changes in the neutral wind and plasma density distribution patterns. While the present paper deals with the observed changes in the MLT region associated with the eclipse more detailed analysis is called for by taking these measured parameters as inputs to the electrojet models as applied to Indian longitudes. Further work on these lines is under progress.

4. Summary

The ENWi probe had been flown on multiple rockets during the recent annular solar eclipse event on 15 January 2010 that passed through the rocket range during afternoon hours when the EEJ intensity is usually high making the first of its kind simultaneous measurements of neutral winds and electron density during an annular solar eclipse at the equatorial region. The analysis of the ENWi data in association with the HF radar data highlight the eclipse induced changes in both the neutral and electrodynamics that resulted in the occurrence of counter electrojet and blanketing Es layers at elevated altitudes over equator.

Acknowledgements

The solar Eclipse campaign was supported by the Indian national program under CAWSES-INDIA. The active participation by the ATVP division and the TERLS rocket range personnel and the keen interest shown by the VSSC in making the program a success is duly acknowledged. The active participation of the Atmosphere Technology Division of SPL is gratefully acknowledged. R. Sridharan duly thanks CSIR for the emeritus scientist position. The work is supported by the Dept. of Space, Govt. of India.

References

Afraimovich, E.L., Palamartchouk, K.S., Perevalova, N.P., Chernukhov, V.V., Lukhnev, A.V., Zalutsky, V.T., 1998. Ionospheric effects of the solar eclipse of March 9, 1997, as deduced from GPS data. Geophysical Research Letters 25 (4), 465–468, http://dx.doi.org/10.1029/98GL00186.

Anandarao, B.G., Raghavarao, R., 1987. Structural changes in the currents and fields of the equatorial electrojet due to zonal and meridional winds. Journal of Geophysical Research 92 (A3), 2514–2526.

Anandarao, B.G., Raghavarao, R., Raghavareddi, C.R., 1977. Electric fields by gravity waves winds in the equatorial ionosphere. Journal of Geophysical Research 82 (10), 1510–1512.
Balsley, B., Rey, A., Woodman, R., 1976. On the plasma instability mechanisms responsible for Esq. Journal of Geophysical Research 81 (7), 1391–1396.
Chandra, H., Som Sharma, P.D., Lele, G., Rajaram, Hanchinal, A., 2007. Ionospheric measurements during the total solar eclipse of 11 August 1999. Earth Planets Space 59, 59–64.
Farley, D.T., Balsley, B.B., 1973. Instabilities in the equatorial electrojet. Journal of Geophysical Research 78, 227–239.
Farley, D., Ierkic, H., Fejer, B., 1981. The absolute scattering cross section at 50 MHz of equatorial electrojet irregularities. Journal of Geophysical Research 86 (A3), 1569–1575.
Fejer, B.G., Kelley, M.C., 1980. Ionospheric irregularities. Reviews of Geophysics and Space Physics 18, 401–454.
Kato, S., 1973. Electric field and wind motion at the magnetic equator. Journal of Geophysical Research 78 (4), 757–762, http://dx.doi.org/10.1029/JA078i004p00757.
Klobuchar, J.A., Whitney, H.E., 1965. Ionospheric electron content measurements during a solar eclipse. Journal of Geophysical Research 70 (5), 1254–1257.
Manju, G., Viswanathan, K.S., Ravindran, S., 2005. Spatial and temporal variations of small scale plasma turbulence parameters in the equatorial electrojet: HF and VHF radar observational results. Annales Geophysicae 23, 1165–1173, http://dx.doi.org/10.5194/angeo-23 1165–2005.
Manju, G., Viswanathan, K.S., 2007. VHF radar studies of counter electrojet events during the northern winter solstice period of 1992. Earth Planets Space 59, 259–265.
Manju, G., Sridharan, R., Sreelatha, P., Sudha, Ravindran, Madhav, M.K., Haridas, Tarun K, Pant, P., Pradeep Kumar, R., Thampi, Satheesh, Neha, Naik, Mridula, N., Lijo, Jose, Sumod, S.G., 2012. A novel probe for in-situ electron density and neutral wind (ENWi) measurements in the near earth space. Journal of Atmospheric and Solar-Terrestrial Physics http://dx.doi.org/10.1016/j.jastp.2011.10.004, ISSN 1364-6826.
Madhav Haridas, M.K., Manju, G., 2012. On the response of the ionospheric F region over Indian low-latitude station Gadanki to the annular solar eclipse of 15 January 2010. Journal of Geophysical Research 117, A01302, http://dx.doi.org/10.1029/2011JA016695.
Muller-Wodarg, I.C.F., Aylward, A.D., Lockwood, M., 1998. Effects of a mid-latitude solar eclipse on the thermosphere and ionosphere—a modelling study. Geophysical Research Letters 25 (20), 3787–3790.
Larsen, M.F., 2002. Winds and wind shears in the mesosphere and lower thermosphere. Journal of Geophysical Research 107, A8 10.109/2001JA000218.
Le, H., Liu, L., Yue, X., Wan, W., Ning, B., 2009. Latitudinal dependence of the ionospheric response to solar eclipses. Journal of Geophysical Research 114, A07308, http://dx.doi.org/10.1029/139 2009JA014072.
Prakash, S., Subbaraya, B.H., Gupta, S.P., 1972. Rocket measurements of ionisation irregularities in the equatorial ionosphere at Thumba and identification of plasma irregularities. Indian Journal of Radio Space Physics 1, 72.
Raghavarao, R., Anandarao., B.G., 1980. Vertical winds as plausible casue for counter electroject. Geophysical Research Letters 7, 357–361.
Reddy, C.A., 1977. The equatorial electrojet and the associated plasma instabilities. Journal of Scientific and Industrial Research 36 (11), 580–589.
Shirke, J.S., Sridharan, R., 1979. On the origin of blanketing and diffuse sporadic E layers at equatorial and low latitudes, low latitude aeronomical processes. Advanced Space Exploration 8, 87–90.
Somayajulu, V.V., Ligi, Cherian, Rajeev, K., Ramkumar, Geetha, Raghavareddit, C., 1993. Mean winds and tidal components during counter electrojet events. Geophysical Research Letters 20 (14), 1443–1446.
Sridharan, R., Devasia, C.V., Jyoti, N., Tiwari, Diwakar, Viswanathan, K.S., Subbarao, K.S.V., 2002. Effects of solar eclipse on the electrodynamical processes of the equatorial ionosphere: A case study during 11 August 1999 dusk time total solar eclipse over India. Annales Geophysicae 20, 1977–1985, http://dx.doi.org/10.5194/angeo-20-1977-2002.
Stening, R.J., Meek, C.E., Manson, A.H., 1996. Upper atmosphere wind systems during reverse equatorial electrojet events. Geophysical Research Letters 23 (22), 3243–3246, http://dx.doi.org/10.1029/96GL02611.
St.-Maurice, J.P., Ambili, K.M., Choudhary, R.K., 2010. Local electrodynamics of a solar eclipse at the magnetic equator in the early afternoon hours. Geophysical Research Letters 38 (L04), 102–105.
Subbaraya, B.H., Satya Prakash, Gupta, S.P., 1983. Electron Densities in the Equatorial Lower Ionosphere From the Langmuir Probe Experiments Conducted at Thumba During the Years 1966–1978. Scientific Report. Indian Space Research Organisation. ISRO-PRL-SR-15–83.
Sumod, S.G., Pant, T.K., Vineeth, C., Hossain, M.M., Antonita, M., 2011. Response of the tropical mesopause to the longest annular solar eclipse of this millennium. Journal of Geophysical Research 116, A06317, http://dx.doi.org/10.1029/2010JA016326.
Tiwari, D., Patra, A.K., Viswanathan, K.S., Jyothi, N., Devasia, C.V., Subbarao, K.S.V., Sridharan, R., 2003. Simultaneous radar observation of electrojet plasma irregularities at 18 MHz and 54.95 MHz over Trivandrum. Journal of Geophysical Research 108 (A10), 1368.
Vineeth, C., Pant, T.K., Sridharan, R., 2009. Equatorial counter electrojects and polar stratospheric sudden warmings—a classical example of high latitude-low latitude coupling? Annalen Geophysicae 27, 3147–3153.
Vineeth, C., Pant, T.K., Devasia, C.V., Sridharan, R., 2007. Highly localized cooling in daytime mesopause temperature over the dip equator during counter electrojet events: first results. Geophysical Research Letters 34, L14101, http://dx.doi.org/10.1029/2007GL030298.
West, K.H., Goldsmith, G., Campbell, D., Zandstra, S., 2008. Effects of the 16 February 1980 solar eclipse on the composition of the low-latitude ionosphere as seen by atmosphere explorer E. Journal of Geophysical Research 113, A12308, http://dx.doi.org/10.1029/2007JA012997.